Polymer 50 (2009) 286–295

Contents lists available at ScienceDirect

Polymer

journal homepage: www.elsevier.com/locate/polymer

Influence of pre-shearing on the crystallization of an impact-resistant polypropylene copolymer

Shijie Song [a], Peiyi Wu [a], Jiachun Feng [a,*], Mingxin Ye [a,b], Yuliang Yang [a]

[a] Key Laboratory of Molecular Engineering of Polymers of Ministry of Education, Department of Macromolecular Science, Laboratory of Advanced Materials (LAM), Fudan University, Shanghai 200433, China
[b] Department of Materials Science, Fudan University, Shanghai 200433, China

ARTICLE INFO

Article history:
Received 21 May 2008
Received in revised form
23 September 2008
Accepted 28 October 2008
Available online 8 November 2008

Keywords:
Pre-shear
Crystallization
Impact-resistant polypropylene copolymer

ABSTRACT

Impact-resistant polypropylene copolymer (IPC) samples with various pre-shear histories were prepared by a Brabender Rheometer. The influence of pre-shearing on crystallization of IPC, including isothermal and nonisothermal crystallization behaviors was investigated by differential scanning calorimetry (DSC) and polarized optical microscopy (POM). The results of nonisothermal crystallization showed that compared with as-received IPC, the temperatures referred to the peak of crystallization exotherm, T_p, were prominently elevated for pre-sheared IPC. In isothermal crystallization experiment, combining Avrami Method and Hoffman–Lauritzen Model, it was found that the half-time of crystallization ($t_{1/2}$) of pre-sheared IPC was greatly shortened and the calculated fold surface free energy (σ_e) within the isothermal temperatures investigated showed a large reduction. Morphological development during isothermal crystallization observed by POM clearly confirmed that the enhancement in crystallization is mainly due to the fast formation of nuclei during crystallization. Besides, using successive self-nucleation and annealing (SSA) thermal fractionation technique, changes in chain structures induced by pre-shearing were obtained. The relaxation behavior of pre-sheared IPC was also evaluated and it was found that the shear-induced enhancement in crystallization could be relaxed to various extents under annealing conditions.

1. Introduction

Crystallization, which involves the transportation of molecules from disordered liquid to ordered solid state, is an important physical process in polymer science and remains a hot issue for both academy and industry. For semi-crystalline polymeric materials, the crystallization proved to be a key factor for final mechanical properties and therefore much attention has been paid on it. Among all the polymers commercialized, isotactic polypropylene (iPP) is a typical semi-crystalline polymer owing various industrial applications because of its ease of processing, light weight, chemical resistance and relatively low cost. However, the poor impact resistance of iPP, particularly at low temperatures, limits its use as an engineering plastic. Many efforts have been made to modify its mechanical properties through physical or chemical methods, for instance, blending with various elastomers [1–4], adding nucleating agents [5–7] and copolymerizing with ethylene-alpha-olefins [8]. In recent years, with the advancement of catalyst and polymerization technology, a new polymeric material called impact-resistant polypropylene copolymer (IPC) has emerged. IPC is produced in-reactor by a multistage polymerization process based on the spherical catalyst [9–11]. The process involves bulk polymerization of propylene in the first stage and then gas-phased copolymerization of ethylene and propylene in the second stage. In comparison with traditional iPP/EPR (ethylene–propylene rubber) prepared by mechanical blending, the elastomer phase dispersed in IPC can be well distributed, which helps to provide much higher impact strength. Previous investigation of the composition and chain structure showed that IPC was composed of iPP homopolymer, which was the main constituent, and of an EPR phase, as well as of partially crystalline ethylene–propylene copolymers [12]. The complicated composition suggests the multi-component and multi-phase nature of IPC.

During thermoplastic processing (e.g. blending and extrusion), polymer crystallization is rarely occurring under static condition. Polymers are usually heated to a molten state and experience both flow and shear for a certain time. After the cessation of flow and shear, polymers will be cooled down by water or air. Therefore, the crystallization behavior is strongly influenced by the thermo-mechanical history during processing [13]. Varga and Karger–Kocsis [14] firstly experimentally investigated the shear-induced crystallization behavior of iPP by pulling a fiber in melt. The results showed that the melt-shearing achieved by fiber-pulling could

* Corresponding author. Tel.: +86 21 6564 3735; fax: +86 21 6564 0293.
E-mail address: jcfeng@fudan.edu.cn (J. Feng).

0032-3861/$ – see front matter © 2008 Elsevier Ltd. All rights reserved.
doi:10.1016/j.polymer.2008.10.054

yield α-row-nuclei and within a specific crystallization temperature interval these α-row-nuclei may induce α to β-transition in the crystalline modification of the iPP. In recent years, many experimental results [13,15–23] have confirmed that flow field applied on molten polymer may strongly affect the orientation of molecules. Hsiao et al. [18] used transmission electron microscope to observe the crystallization morphology of iPP after shear and found the formation of micron size fibrillar (thread-like) structures at the instant of flow cessation. These fibrillar structures were considered as some oriented polymer chains and could act as nuclei for subsequent crystallization. These oriented molecules proved to have a long lifetime [13,18,21,23–26]. If the oriented molecules fail to completely relax themselves within the period between the cessation of flow and subsequent cooling, they will be remained stable in matrix. They could induce specific crystallization morphology (i.e. shish–kebab) under some circumstances and open a new kinetic pathway to nucleation. Therefore, melt-processed polymers may exhibit totally different crystallization kinetics. The study of this flow-induced crystallization (FIC) on semi-crystalline polymers makes it possible to control and predict the final properties. The commercial importance of FIC has long been recognized. Nevertheless, the understanding of FIC is not an easy task for researchers. Usually, there are two methods to study FIC: (i) by practical processing operation such as an extruder which reproduces industrial processing conditions with a wide distribution of shear rates in a pressure-driven slot flow; (ii) by experiments performed under controlled thermal and flow conditions in a laboratory rheometer [27]. Nowadays, with in situ rheo-optic, rheo-SAXS (small-angle X-ray scattering) and rheo-WAXD (wide-angle X-ray diffraction) techniques, real-time tracking the FIC phenomenon can also be performed to provide a better understanding of the process [17,20,21,28,29].

A relatively clear overview of FIC [18,19,25] has been given in recent years especially for some homogeneous polymer systems such as iPP. In addition to experimental studies, a series of models to numerically predict the crystallization process of homogeneous polymer system under flow have also been proposed [30–35]. However, compared with homogeneous system, fewer studies have been focused on the heterogeneous system. As a typical multi-component and multi-phase polymer, IPC has gained much attention on its composition, microstructure and morphology [36,37]. Nevertheless, the experimental and theoretical work on FIC of IPC is relatively less reported in the literatures [38] and has not been well investigated up to now. The flow-induced crystallization of a multi-phase polymer is more complicated as well as interesting because it may be related to not only shear but also the phase separation [39]. Undoubtedly, it is of great importance to understand the FIC of IPC, which may reflect the responses of internal complex structures to an external flow field. Therefore, the objective of this paper is to study how pre-shearing influences the crystallization kinetics of a commercial IPC. The IPC samples with different pre-shear histories were prepared and the influence of shear rate, duration time on both isothermal and nonisothermal crystallization was studied by differential scanning calorimetry (DSC). The morphological development during isothermal crystallization was observed by polarized optical microscopy (POM). To further explore the crystalline structure, successive self-nucleation and annealing (SSA) fractionation was applied. We also reported a relaxation behavior of pre-sheared IPC and evaluated it by annealing under different conditions.

2. Experimental

2.1. Material and sample preparation

Material used in this investigation is a commercial-grade impact-resistant polypropylene copolymer with granule form. It was kindly provided by Qilu Petrochemical Co., SINOPEC (Shangdong, China). The weight-average molecular weight was 1.53×10^5 and the polydispersity index (M_w/M_n) was 5.02, determined by gel permeation chromatography (GPC). The ethylene content of IPC was 10.6wt% as determined by ^{13}C NMR. Dynamic mechanical analysis (DMA) showed two glass transition temperatures existed in IPC at about −32.8 °C and 23.6 °C corresponding to the relaxation of rubber phase and iPP matrix, respectively. The onset degradation temperature of IPC was 260.0 °C in air atmosphere measured by thermogravimetric analysis (TGA) at a heating rate of 20 °C/min.

Pre-shearing was carried out by a Brabender Rheometer (PLE 651) to simulate the practical industrial processing. As-received IPC pellets were carefully weighted to fill in the chamber without adding any nucleating agents or additives and subsequently heated to 170 °C. To obtain samples of different pre-shear histories, various rotor speed (5–40 rpm) and duration time (5–15 min) were applied. As soon as the duration of pre-shearing reached a preset time, we stopped both rotation and heating of the rheometer and opened a water-circulation cooling system which was directly connected to the chamber. The samples left in the chamber were cooled to room temperature by water-circulation and then scratched out for further measurement. The room temperature was kept at 25 °C by air-conditioning. The temperature of material in the chamber can be recorded by a sensor attached and the corresponding heating or cooling curve (temperature–time curve) can be analyzed by the software attached in computer. In this study, all the samples were prepared under the same cooling condition. According to the temperature–time curves obtained it was confirmable that the heating and cooling rates could be identical for different samples' preparation to ensure the comparison between samples.

For torque rheometer consisted of chamber and rotor with given geometry and size, the shear rate, $\dot{\bar{\gamma}}$, is in direct proportion to the rotor speed [40,41]. According to the studies of Nielsen [42] and Nakajima and Harrel [43], the shear rate in an internal mixing head can be calculated as follows: $\dot{\bar{\gamma}} = R\omega_r/e$, where $\dot{\bar{\gamma}}$ is the shear rate (s^{-1}), R is the radius of rotor (mm), ω_r is the angular velocity of the rotor (rad/s), and e is the distance between the rotor and chamber (mm). For the rotor (model MB30H, attached to Brabender) used in this study, $R = 21.0$ mm, $e = 2.0$ mm, and $\omega_r = 2\pi\omega/60$, thus the shear rate can be expressed mathematically as follows: $\dot{\bar{\gamma}} = 1.10\omega$, where ω is the rotor speed (rpm). Therefore, the rotor speed of 5 rpm, 10 rpm, 20 rpm, 30 rpm, 40 rpm we employed can supply a shear rate of 5.5 s^{-1}, 11.0 s^{-1}, 22.0 s^{-1}, 33.0 s^{-1}, 44.0 s^{-1}, respectively.

2.2. Thermal analysis and thermal fractionation

A Q-100 DSC (TA Instruments-Waters LLC, USA) was used for determining the thermal properties of IPC. Calibration for the temperature scale was performed using indium ($T_m = 156.60$ °C and $\Delta H_f^0 = 28.45$ J/g) as standard to ensure reliability of the data obtained. The accuracy of temperature measured here is ±0.05 °C. All the experiments were carried out in nitrogen atmosphere.

2.2.1. Crystallization and melting behavior characterization

Samples were sealed in aluminum pans for DSC measurements. To minimize the thermal lag between samples and DSC furnace, each sample weighs about 10 mg. The measurements were performed as following procedures: samples were heated to 200 °C at 10 °C/min and kept for 5 min to erase any previous thermal history, then cooled to 25 °C at 10 °C/min to determine the temperature (T_p) at the peak of the exothermic curve. The melting point (T_m) was taken at the melting endotherm peak of the second heating cycle after erasing the thermal history. The melting enthalpy was determined by linear interpolation of the baseline between the

clear-cut end of the melting endotherm and its onset arbitrarily taken at 70 °C for all the samples.

Isothermal crystallization was carried out according to the following procedure: (a) Samples were heated to 200 °C and kept for 5 min to standardize the physical state of the materials prior to the experiment. (b) Fast cooling (50 °C/min) down to a predetermined crystallization temperature (T_c). (c) Isothermally kept for a period of time necessary to complete the crystallization.

2.2.2. SSA thermal fractionation

The SSA used for the thermal treatment of as-received IPC and pre-sheared IPC samples involved a series of heating–annealing–cooling cycles and was performed according to the following procedures: Samples were firstly heated to 200 °C at 10 °C/min and kept for 5 min, then cooling to 25 °C at 10 °C/min to create an initial "standard" thermal history. Secondly, samples were heated to a selected first self-seeding temperature (T_s) at 10 °C/min and maintained at this temperature for 5 min. This step results in partial melting and annealing of unmelted crystals, while some of the melted species may isothermally crystallize. Crystallization after self-nucleation was achieved by subsequently cooling samples to 25 °C at 10 °C/min. The first T_s was determined to be 170 °C for both as-received IPC and pre-sheared IPC samples. The fraction window adopted here was 5 °C, and the annealing time was 5 min. The temperature range for thermal fractionation was from 170 °C to 55 °C at interval of 5 °C for both as-received IPC and pre-sheared IPC samples. The scanning rate used during the thermal conditioning steps was 10 °C/min. After the completion of thermal fractionation process, samples were heated from 25 °C to 200 °C at 10 °C/min and the corresponding endothermic curves were recorded.

2.2.3. Evaluation of relaxation

The relaxation experiments were performed for pre-sheared samples and the measurements were carried out using DSC according to the following procedures: samples were quickly heated from room temperature to 200 °C at a rate of 20 °C/min and then cooled down to 25 °C at a rate of 10 °C/min. The corresponding exothermic curves were recorded to observe the preserved changes of crystallization behaviors caused by pre-shear history. Then the relaxations of samples were evaluated by two methods: (i) samples were heated to 200 °C and annealed for different duration times; (ii) samples were heated to various annealing temperatures above their melting temperatures for the same duration times. After the cessation of annealing, samples were again cooled down to 25 °C at a rate of 10 °C/min and the exotherms were recorded to show the changes of crystallization behaviors after relaxation.

2.3. Polarized optical microscopy

Morphologies of samples were observed using an Olympus BX-51 polarized optical microscope with a Linkam-THMS600 hot stage. The sensor accuracy of the hot stage is ±0.1 °C. Samples were melted at 200 °C and squeezed to films tenderly. These films were kept in the hot stage between two microscope slides. Each sample was heated to 200 °C at 30 °C/min and kept for 5 min to allow complete melting and subsequently cooled to a predetermined isothermal crystallization temperature at 40 °C/min. Nitrogen gas was purged through the hot stage during measurements.

3. Results and discussion

3.1. Thermal properties of IPC

The thermal properties of as-received IPC sample were measured using a standard heating/cooling/heating program by DSC at an identical rate of 10 °C/min. The melting temperature (T_m), the heat of fusion (ΔH_m), the peak crystallization temperature (T_p) and the crystallinity (χ_c) are presented in Table 1. For a better understanding of IPC system, the thermal properties of a commercial iPP (F401, a product of Yangzi Petrochemical Co., SINOPEC), homopolymer with M_w of 4.3×10^5 and isotacticity of 96.5%, were also provided for comparison. Table 1 shows that the melting temperature of as-received IPC was around 165 °C which was very close to that of iPP. For IPC sample, a tiny melting peak can also be observed at about 120 °C, which is said to be the melting point of crystallizable polyethylene segments in ethylene–propylene block copolymer according to literatures [12,44].

Table 1
Thermal properties of IPC studied in this work.

Materials	T_m[a,d] (°C)	ΔH_m[a,d] (J/g)	T_p[b,d] (°C)	$\chi_{c,PP}$[c,d] (%)
As-received IPC	164.66 ± 0.90	79.72 ± 2.32	112.51 ± 0.30	38.15 ± 1.11
iPP	166.68 ± 0.83	107.40 ± 2.54	117.10 ± 0.36	51.38 ± 1.20

[a] Determined from melting endotherm of DSC heating trace after erasing the previous thermal history.
[b] Determined from crystallization exotherm of DSC cooling trace after melted.
[c] Determined from measured enthalpies of fusion, $\Delta H_m(\Delta H_m^0 = 209.0$ J/g).
[d] Mean values of three measurements.

The peak crystallization temperature (T_p) is widely used to evaluate the crystallization ability of semi-crystalline polymer. For as-received IPC, T_p appeared to be at about 112 °C, which was lower than iPP indicating that IPC may exhibit a slower crystallization rate. With regard to the crystallinity, IPC owns a much lower value than iPP due to the existence of amorphous ethylene–propylene random copolymers. These results clearly showed that IPC studied here was a complex system containing iPP homopolymers, ethylene–propylene random copolymers and ethylene–propylene block copolymers with crystallizable polyethylene segments. Our interests lie in how the crystallization behavior of this complicated material changes in response to different pre-shear histories, the results of which may be helpful for giving meaningful information to practical production as well as laboratory research. Therefore, much attention has been paid on these aspects in this study.

3.2. Effect of pre-shearing on nonisothermal crystallization of IPC

Fig. 1 shows the nonisothermal crystallization curves of as-received IPC and IPC samples after pre-shearing for 5 min under various rates (5.5–44.0 s^{-1}). The evident change in these

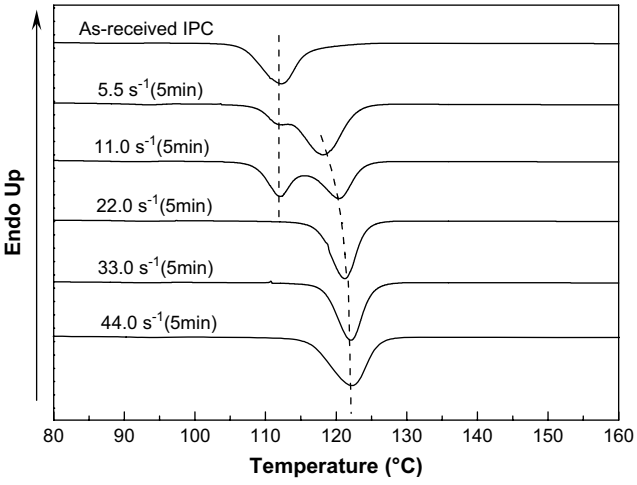

Fig. 1. Effect of pre-shearing rate on nonisothermal crystallization behaviors of IPC. The shear temperature was 170 °C.

exothermic curves suggested that shear rates greatly influenced the nonisothermal crystallization behaviors of IPC. The as-received IPC shows a single exothermic peak ($T_p = 112$ °C) on DSC crystallization traces. However, the IPC sample pre-sheared under 5.5 s^{-1} shows double exothermic peaks, a main exothermic peak at about $T_p = 118$ °C and a shoulder peak at $T_p = 112$ °C. Obviously the exothermic peak at 112 °C could be regarded as the crystallization of some as-received IPC components hardly affected by pre-shearing. The peak at 118 °C was referred to the enhanced crystallization which might be induced by some oriented molecules formed during pre-shearing. At low shear rate, because of the shear gradients and limited duration time, only part of the polymer melt underwent sufficient shear and stretch, the others were just slightly moved. Therefore, after the cessation of flow, two components with different shear histories remained and the sample exhibited bimodal exotherms during the subsequent nonisothermal crystallization. When applied shear rate was elevated to 11.0 s^{-1}, the exothermic peak at 112 °C could still be observed. However, the other exothermic peak was further moved to 120 °C indicating that with higher shear rate the orientation of molecules was strengthened leading to a higher T_p. With regard to 22.0 s^{-1}, the exothermic peak at 112 °C disappeared and only one exothermic peak ($T_p = 121$ °C) could be observed. The results obtained at 33.0 s^{-1} and 44.0 s^{-1} were almost same and one exothermic peak at about 122 °C was observed, which implied that the elevation of T_p reached a maximum under these pre-shearing conditions.

The influence of pre-shearing duration on the nonisothermal crystallization of IPC was also evaluated and shown in Fig. 2. All the samples were applied same shear rate (11.0 s^{-1}) but with different duration times (5–15 min). When the duration of pre-shearing lasted for 5 min, a bimodal exotherm could be obtained, one T_p at 112 °C obviously corresponding to the crystallization of as-received IPC sample and the other at 120 °C corresponding to the crystallization induced by oriented molecules. If the duration time was extended to 10 min, the exothermic peak at 112 °C disappeared and only a single exothermic peak ($T_p = 121$ °C) could be observed. Further prolonging the duration to 15 min made T_p to move to a slightly higher temperature at 122 °C.

In brief, by controlling the pre-shearing condition, IPC samples with different crystallization behaviors could be obtained. It is clear that both pre-shearing rate and duration time have strong influences on the subsequent crystallization behavior of IPC. With different pre-shear histories, the T_p of IPC changed and moved to higher temperatures. If sufficient high shear rate or enough duration time was applied, the T_p could reach a potential maximum value at 122 °C which was almost 10 °C higher than that of as-received IPC. The elevation of T_p indicated a surprising faster crystallization rate. Usually, such a great enhancement of crystallization may be achieved by adding effective nucleating agents. However, according to our study, the same enhancement could also be realized by proper pre-shearing.

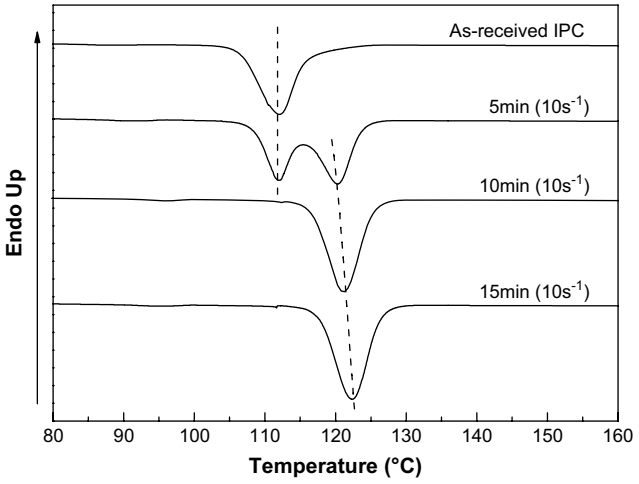

Fig. 2. Effect of pre-shearing duration time on nonisothermal crystallization behavior of IPC. The temperature was 170 °C.

3.3. Effect of pre-shearing on isothermal crystallization kinetics

To further confirm the faster crystallization enhanced by pre-shearing, the isothermal crystallization behaviors of as-received IPC and pre-sheared samples were comparatively investigated. It should be noted first that the pre-sheared samples used in the following measurements were prepared by undergoing a shear history of 33.0 s^{-1} and 10 min whose T_p proved to reach the maximum value of 122 °C.

The isothermal crystallization temperature should be well chosen to ensure the feasibility of the measurements and the integrality of the data obtained. For as-received and pre-sheared IPC samples studied here, according to our measurements, on the one hand, if lower crystallization temperature (≤128 °C) is chosen, the isothermal crystallization of pre-sheared IPC will be so fast that only part of the exothermic curve could be recorded because the sample starts to crystallize before the selected crystallization temperature is reached. On the other hand, isothermal crystallization at higher temperatures (≥136 °C) will be time-consuming for as-received IPC and unsuitable for laboratory investigation. Therefore, temperatures ranging from 129.0 to 135.0 °C were considered to be appropriate for the isothermal crystallization investigations in this study.

The relative degrees of crystallinity (X_t) changing with crystallization time at 129.0 °C, 131.0 °C, 133.0 °C and 135.0 °C are shown in Fig. 3. The corresponding exothermic DSC curves at these temperatures are also presented in the inset of Fig. 3. The X_t here is a relative value and could be defined as follows.

$$X_t = \int_0^t (dH/dt)dt / \int_0^\infty (dH/dt)dt \quad (1)$$

where the first integral is the heat generated at time t and the second one is the total heat generated when the crystallization is completed.

It can be seen From Fig. 3 that, both as-received IPC and pre-sheared IPC samples showed an obvious dependence of crystallization temperature on isothermal crystallization rate. Amazingly, under the same isothermal crystallization temperature, the pre-sheared IPC sample took much shorter time to complete the crystallization than as-received sample. For instance, at 129 °C, the pre-sheared IPC sample completed crystallization in 2–3 min while the as-received sample spent as long as about 30 min. Moreover, the enhancement of crystallization rate appeared to be more pronounced under higher crystallization temperatures.

We used the Avrami model, whose logarithmic form is expressed as Eq. (2), to analyze the isothermal crystallization of these IPC samples [45].

$$\ln[-\ln(1 - X_t)] = \ln K_n + n \ln t \quad (2)$$

where K_n is the kinetic growth rate constant, n is the Avrami exponent related to the type of nucleation and to the geometry of growing crystals. Fig. 4 gives the Avrami plots corresponding to as-received IPC and pre-sheared IPC. From the slope and intercept of these straight lines, the Avrami exponent n and the rate constant $K_n(T)$ can be obtained. Further, the half-time of crystallization, $t_{1/2}$, defined as the time at which the development of crystallization is

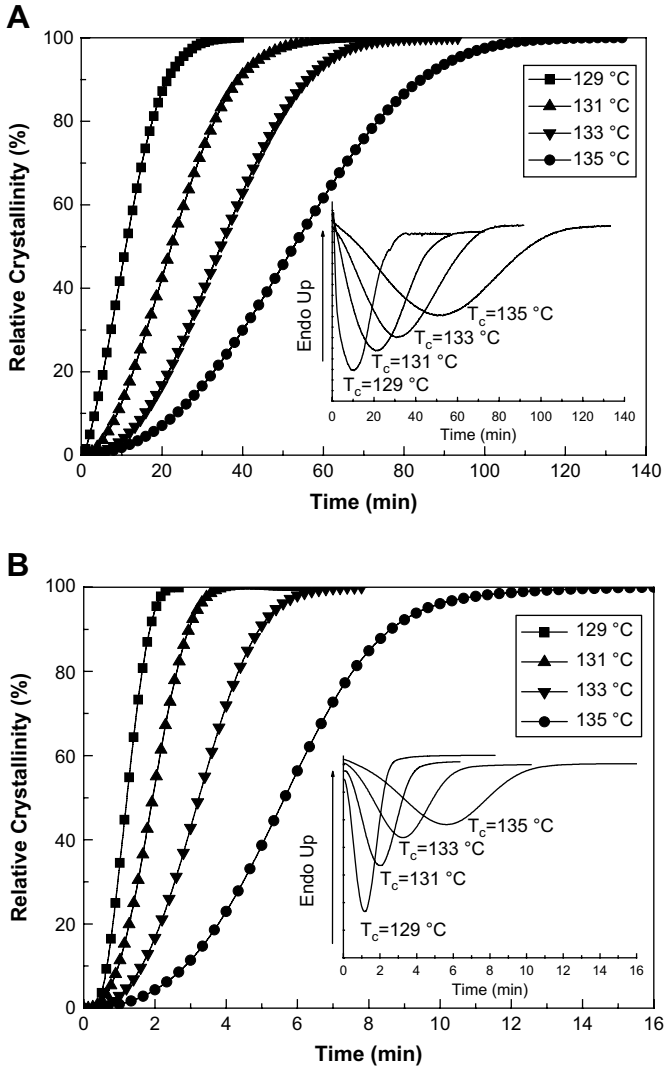

Fig. 3. Plots of relative crystallinity versus crystallization time for (A) as-received IPC and (B) pre-sheared IPC when isothermally crystallized at 129.0 °C, 131.0 °C, 133.0 °C and 135.0 °C. Inset gives the corresponding exothermic DSC curves at these temperatures.

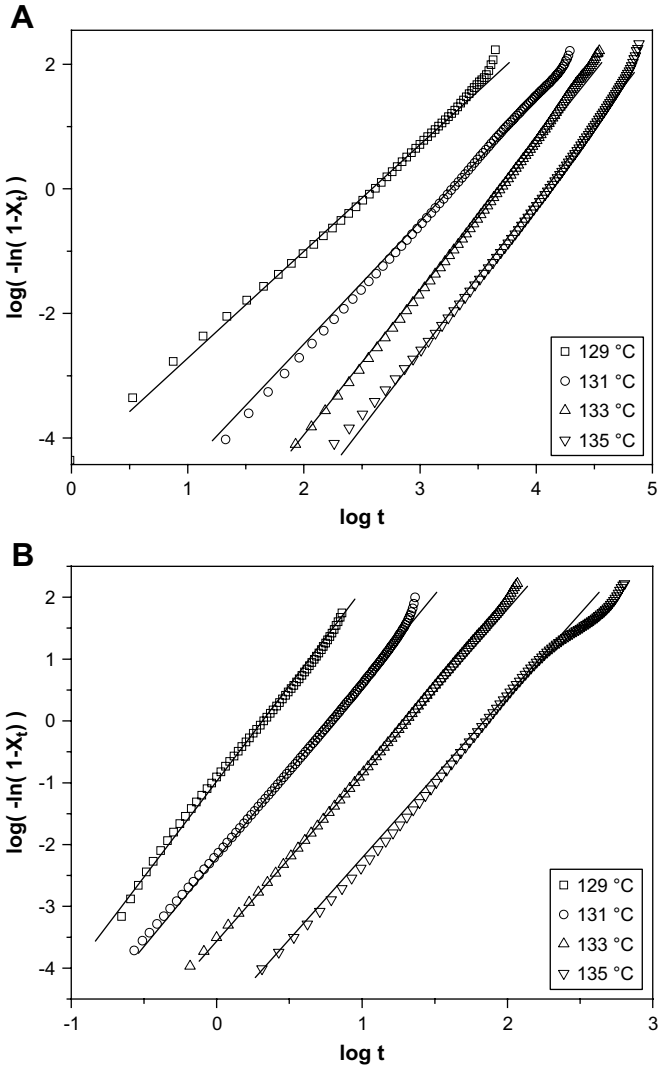

Fig. 4. The Avrami plots corresponding to (A) as-received IPC sample and (B) pre-sheared IPC sample.

50% complete, can be determined from $K_n(T)$ and n as $t_{1/2} = (\ln 2/K_n(T))^{1/n}$. In isothermal crystallization, $t_{1/2}$ is usually used to evaluate the crystallization rate.

The values of n, $K_n(T)$ and $t_{1/2}$ of two samples at various temperatures are listed in Table 2. It is evident that, when compared $t_{1/2}$ of two samples, the pre-sheared IPC exhibited a remarkable faster crystallization rate under all isothermal crystallization temperatures. For example, the $t_{1/2}$ was shortened by 88.6% at 129 °C. With the results of overall crystallization rates, we may come to the conclusion that the pre-shearing process can greatly accelerate the crystallization of IPC. From Table 2 it can also be seen that the n values of as-received IPC are dispersed, ranging from 2.07 to 2.41 whereas the n values of pre-sheared IPC are relatively larger than as-received IPC, ranging from 2.73 to 3.02. We believe that the pre-sheared induced changes in Avrami exponent were related to the microstructure of two samples. The different microstructures lead to the different nucleation mechanisms.

Besides, the effect of pre-shearing on the crystallization kinetics of IPC is also reflected in the fold surface free energy of IPC crystals. The fold surface free energy, σ_e, is usually obtained by measuring the variation of linear growth rate of spherulites, G, with temperature. Hoffman and Lauritzen (H–L) had developed a dependence of G on the crystallization temperature T_c [46], that is

$$G = G_0 \exp\left[\frac{-U^*}{R(T_c - T_0)}\right] \exp\left[\frac{-K_g}{T_c(\Delta T)f}\right] \quad (3)$$

Table 2
The Avrami exponent (n), crystallization half-time ($t_{1/2}$), and overall crystallization rate ($K_n(T)$), of as-received IPC and pre-sheared IPC samples at various crystallization temperatures (T_c).

Samples	T_c (°C)	$K_n(T)$ (min^{-n})	n[a]	$t_{1/2}$[b] (min)
As-received IPC	129.0	3.60 E-03	2.07	11.38
	131.0	1.13 E-03	2.16	22.27
	133.0	1.38 E-04	2.41	34.35
	135.0	5.55 E-05	2.39	51.78
Pre-sheared IPC	129.0	0.3791	3.02	1.22
	131.0	0.1119	2.79	1.92
	133.0	2.87 E-02	2.73	3.21
	135.0	5.51 E-03	2.80	5.62

[a] Mean value of three measurements. Calculated standard deviation of n is within ±0.1.
[b] Calculated from the mean value of n.

where G_0 is a constant and includes all the terms that are temperature-insensitive, U^* is the transport activation energy, T_0 is a hypothetical temperature below which all viscous flows cease (namely, $T_0 = T_g - 30$ K), T_c is the crystallization temperature, $\Delta T = T_m^0 - T_c$ is the undercooling (T_m^0 is the equilibrium melting temperature), f is the correction factor related to temperature usually described as $f = 2T_c/(T_m^0 + T_c)$. The factor $\exp[-U^*/R(T_c - T_0)]$ describes the rate of transport of chain segments to the growth front and dominates the behavior of G below the maximum in the growth rate. The factor $\exp[-K_g/T_c(\Delta T)f]$ dominates the variation of G near T_m^0 and well down toward the maximum in the growth rate. The nucleation constant in Eq. (3), K_g can be expressed as:

$$K_g = jb_0\sigma\sigma_e T_m^0/k_B\left(\Delta h_f\right) \tag{4}$$

where $j = 4$ for regimes I and III growth and $j = 2$ for regime II. b_0 is the layer thickness, σ is the lateral surface free energy, Δh_f is the enthalpy of fusion, k_B is Boltzmann's constant. Under different temperatures, the crystallization of polymer can be divided into three regimes by the relationship between lateral growth rate g and second nucleating rate i: Regime I ($i < g$), Regime II ($i \cong g$) and Regime III ($i > g$). To confirm the value of j in this study, we performed more isothermal crystallization experiments in a wider range of isothermal temperatures and drew the H–L plots. The related results were available in Supporting materials attached. It was showed that within the isothermal temperature used here (129–135 °C), the crystallization of as-received sample was in regime II while the pre-sheared IPC was in regime III. Therefore, the value of j was 2 for as-received IPC and 4 for pre-sheared IPC in the calculation of σ_e. When the Avrami equation to describe the overall crystallization of the whole sample is combined with the crystal growth rate equation of L–H, the overall crystallization rate could be expressed by a generalized equation as follows [47]:

$$\frac{1}{n}\ln K_n(T) + \frac{U^*}{R(T_c - T_\infty)} = A_n - \frac{K_g}{T_c(\Delta T)f} \tag{5}$$

where $K_n(T)$ and n are the parameters in the Avrami equation, others are from Eq. (3). Therefore, K_g of two samples can be determined from the slope of plot of $1/n \ln K_n(T) + U^*/R(T_c - T_\infty)$ versus $1/fT_c(\Delta T)$ and σ_e can be obtained from $\sigma\sigma_e$ by substituting K_g into Eq. (4). In addition, to determine the value of σ_e, it is first necessary to determine σ, which could be calculated from the following empirical equation.

$$\sigma = \alpha\Delta h_f\sqrt{a_0 b_0} \tag{6}$$

where α is an empirical constant and usually assumed to be 0.1, $a_0 b_0$ represents the cross-sectional area of polymer chains. Δh_f, a_0 and b_0 of PP is supposed to be 1.96×10^8 J m^{-3}, 5.49×10^{-10} m and 6.26×10^{-10} m, respectively, based on the literature [48]. Therefore, a value of $\sigma = 11.5$ erg cm^{-2} is obtained from Eq. (6).

On the basis of above results, the values of σ_e can be calculated from Eq. (4). Within the isothermal crystallization temperatures studied, the values of σ_e calculated for as-received IPC and pre-sheared IPC are 116.5 erg cm^{-2} and 76.6 erg cm^{-2}, respectively. These values are higher than those of iPP reported in the literature [48–51] whose values fall in the range 58 ± 7 erg cm^{-2} which may be due to the complexity of IPC system. Compared the values of σ_e for two samples, it is evident that the pre-shearing process gives rise to the decrease in σ_e of as-received IPC. Usually, it is believed that the value of σ_e could be changed by nucleating agents such as filler particles and fibers. These additives tend to promote the nucleation of spherulites on their surfaces, decrease the thickness of lamina and lead to epitaxial growth of the crystallites [52]. As a result, the value of σ_e is reduced, thereby giving rise to an increase in crystallization rate. In our experiment, a 34% reduction in σ_e of as-received IPC indicating that pre-shearing may have similar effects as nucleating agents. Therefore, we estimate that the flow field applied to as-received IPC greatly enhanced the nucleation process which leads to a surprisingly faster overall crystallization rate.

3.4. Morphological observation of as-received IPC and pre-sheared IPC samples

To confirm the existence of faster nucleating phenomenon in pre-sheared IPC, the morphology development and size of spherulites of as-received IPC and pre-sheared IPC samples were investigated by polarized optical microscopy (POM). Equipped with a hot stage, real-time isothermal crystallization process could be observed and morphologies during the process could be photographed. As we have shown before, the pre-sheared IPC sample exhibited a much faster crystallization rate than as-received IPC; therefore the undercooling should be well selected to ensure a proper time window for the observation of both as-received IPC and pre-sheared IPC. As isothermal crystallization kinetic studies were tested under 129–135 °C, we selected a temperature of 135 °C for optical observation here to compare with the former results and the temperature proved to be appropriate.

Fig. 5 displays the morphological evolution of as-received IPC and pre-sheared IPC during the isothermal crystallization at 135 °C. It can be seen that at 1 min which was just at the beginning of isothermal crystallization, the as-received IPC sample remained a homogeneous phase that almost no nuclei could be observed. However, with regard to the pre-sheared sample, some sporadic nuclei were already visible at 1 min indicating that the germination of the sample was much earlier than that of as-received sample. At 3 min, it was clear that some nuclei emerged in as-received sample while in pre-sheared sample the germination of nuclei was so rapid that the screen had already been full of nuclei and the small spherulites began to impinge on each other. After 10 min of isothermal crystallization, it can be seen that no more nuclei appeared in as-received IPC sample and the formed spherulites began to grow radially. For pre-sheared IPC sample, the crystallization had already gone saturation by 10 min because compared with the photo taken at 25 min, no distinct differences were found. However, the crystallization of as-received sample took about 25 min to reach saturation. It can also be estimated that the spherulites' size of pre-sheared sample was much smaller than that of as-received sample when the two samples both reached saturation. For pre-sheared sample, the nuclei germination was much earlier and nuclei density was much higher at the same crystallization time. Under the same crystallization temperature, the number of nuclei formed during a limited crystallization time may represent the nucleation rate of the sample [53]. Therefore, it is clear that the nucleation rate of pre-sheared IPC sample showed a significant promotion compared to as-received IPC. In the former isothermal study at 135 °C, using Avrami method and H–L approach, we have estimated that the σ_e of pre-sheared samples was lower than those of not pre-sheared samples which means that the nucleation rate ought to be higher in pre-sheared samples. Therefore, the results of isothermal study and optical observation were well corresponded indicated that the faster germination (nucleation rate) was the main reason for crystallization acceleration of pre-sheared IPC.

3.5. Thermal fractionation

Successive self-nucleation and annealing (SSA) thermal fractionation enhances the potential molecular fractionation which can occur during crystallization, while encouraging annealing of the

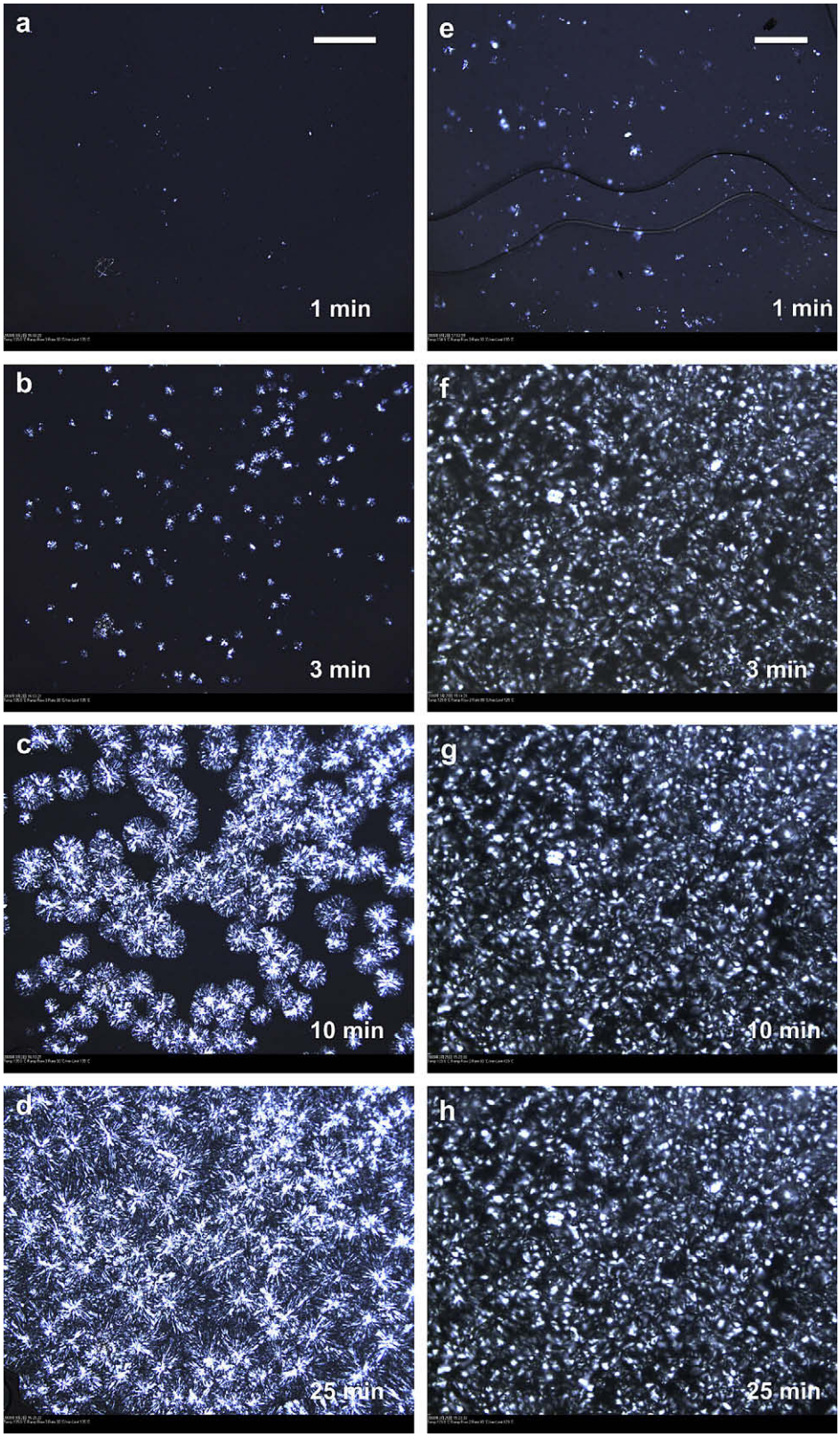

Fig. 5. Morphologies development of as-received IPC (a–d) and pre-sheared IPC (e–h) during isothermal crystallization.

unmelted crystals at each stage of the process, so that small effects can be magnified. This technique is based on the sequential application of self-nucleation and annealing steps to a polymer sample originally devised by Fillon et al. [54–56] and has been widely used to analyze the chain structures of semi-crystallized polymers such as PE and PP [57–62]. For an SSA fractionated polymer sample, the final DSC heating run will reveal a distribution of melting points induced by thermal treatment indicating the heterogeneous nature

of the structures of polymers. Compared with another thermal fractionation technique so-called stepwise crystallization (SC), SSA exhibits a leading advantage that it is performed at substantially shorter times and with better resolution [63,64].

In order to clarify the microstructure changes of as-received IPC after pre-shearing, SSA thermal fractionation was performed. The DSC melting curves of as-received IPC and pre-sheared IPC after SSA fractionation are shown in Fig. 6. It is evident that, both fractionated samples exhibited a series of small melting peaks at about 90–130 °C which correspond to the partially crystalline ethylene–propylene copolymers. By zooming in these melting peaks, it is found that little difference could be observed between as-received IPC and pre-sheared IPC. However, it is interesting to see that the melting peaks at higher temperatures corresponding to iPP homopolymers were quite different between the two samples. The as-received sample showed two obvious melting peaks, a weak one at 171 °C and a strong one at 177 °C. With regard to the pre-sheared sample, the peak at 177 °C became a weak shoulder of a much stronger peak at 171 °C. The melting peaks of fractionated samples were related to the melting of different mean lamellar thickness crystallites formed and annealed at each self-nucleation temperature employed. The Thomson–Gibbs equation [64] can be used to establish a correlation between temperature and lamellar thickness which has been used by several authors who have applied SSA fractionation.

$$l = \frac{2\sigma T_m^0}{\Delta H_v \left(T_m^0 - T_m\right)} \tag{7}$$

According to Eq. (7), it can be seen that by SSA fractionation, two crystalline components with different mean lamellar thicknesses could be obtained for both samples. The peak position corresponding to the two components showed no differences after pre-shearing indicated that the pre-shearing did not change the lamellar thickness of the two fractionated components. However, the proportion of the two components has been greatly changed. The pre-shearing promoted the formation of thinner lamellar and therefore the melting peak at lower temperature 171 °C became stronger while the peak at 177 °C became weaker. The microstructure of pre-sheared sample proved to be more homogeneous reflected by the crystallizable segment distribution. As we have mentioned, the pre-shearing applied to as-received IPC would lower the Avrami exponent indicating the existence of a microstructure change. With the results of SSA thermal fractionation, we may reach the conclusion that the pre-shearing process has a prominent influence on changing the distribution of lamellar thickness of IPC by forming thinner lamellar. The results were also consistent with its nucleating effect on IPC as we have presented before.

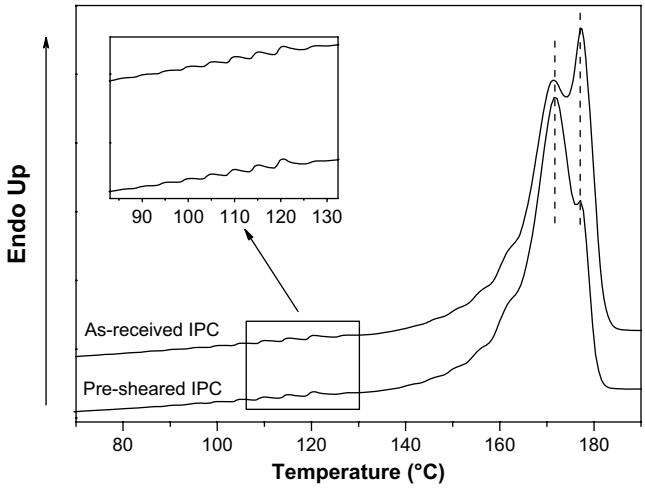

Fig. 6. DSC melting curves of as-received IPC and pre-sheared IPC after SSA thermal fractionation.

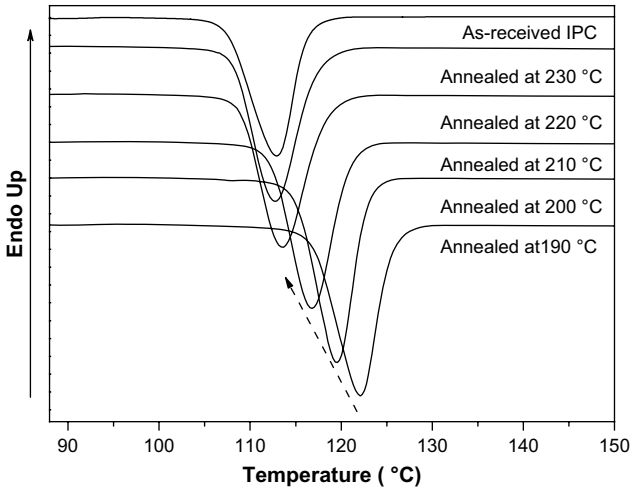

Fig. 7. Exothermic curves of pre-sheared sample after annealing at various temperatures for 30 min.

3.6. Relaxation behaviors of pre-sheared IPC

If the enhancement in crystallization of IPC is caused by pre-shearing related to the orientation of polymer chains (formation of oriented "precursors"), the orientation may be expected to relax under certain conditions. Therefore crystallization characteristics of pre-sheared IPC will be recoverable. The relaxation behavior of pre-sheared polymer involves the motion of oriented or stretched molecules to recover from a metastable state to a stable state. Usually under quiescent condition and room temperature, this process takes such a long time that it is impossible to observe. However, according to the time–temperature correspondence, if the polymer is kept in a high temperature atmosphere, the relaxation process might be easier to observe and record. Therefore, the two methods we adopted in this study to perform the relaxation process of pre-sheared IPC sample were: (i) annealing at different temperatures which were much higher than its melting temperature for a same duration time; (ii) annealing for various duration times at a same temperature. The degrees of relaxation were evaluated through subsequent nonisothermal crystallization by determining the T_p value on exothermic curves.

Fig. 7 presents the exothermic curves of pre-sheared sample after annealing at various temperatures for 30 min. Interestingly, the relaxation was quite obvious and showed a dependence of annealing temperature. From Fig. 7, the T_p of pre-sheared sample exhibited no essential difference implying that the relaxation under 190 °C was so slow that within the limited annealing time, the shear-induced structures could not be destroyed. However, with the increasing annealing temperature, the pre-sheared sample began to show more and more obvious relaxation behaviors which could be inferred from the fact that the T_p of annealed samples moved to lower temperatures. When the annealing temperature was set to 230 °C, the T_p of pre-sheared IPC sample after annealing was identical to that of as-received IPC sample indicating that a sufficient relaxation was achieved and the pre-shearing memory was totally erased.

Fig. 8 shows the exothermic curves of pre-sheared sample after annealing at 200 °C for various duration times. The relaxation

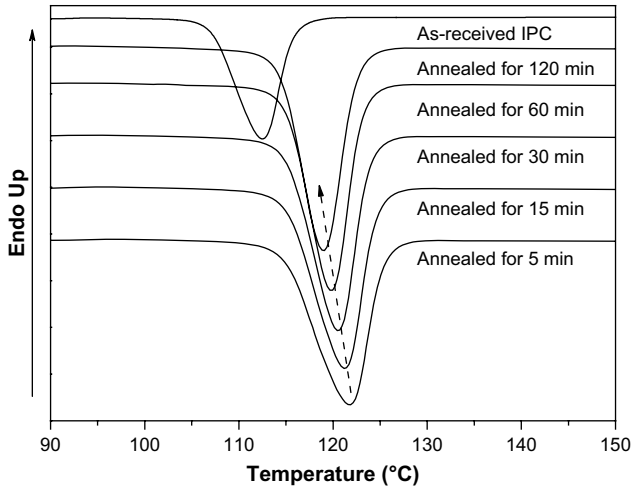

Fig. 8. Exothermic curves of pre-sheared sample after annealing at 200 °C for various times.

behavior also showed a dependence of annealing time under same annealing temperature. Annealing at 200 °C for 5 min is an often used procedure to erase the previous mechanical and thermal histories in thermal analysis. However, according to the result obtained here, this procedure failed to erase the melt memory caused by flow because the subsequent crystallization revealed that the T_p did not show any differences compared with original pre-sheared IPC. When longer annealing time was applied, the pre-sheared samples started to exhibit relaxation behaviors. The observed T_p was 121.1 °C, 120.3 °C, 119.7 °C, 118.8 °C for samples annealed for 15 min, 30 min, 60 min and 120 min, respectively. It shows that annealing for 120 min at 200 °C was not long enough for the stressed melt to relax totally. Therefore, it can be estimated that much longer annealing time need to be applied before the pre-sheared IPC sample recovers to a stable state.

Besides, it should also be noted that the as-received IPC is a multi-phase polymer system composed of homo-polypropylene, ethylene–propylene random copolymer and ethylene–propylene block copolymer. The dispersion of these components is strongly related to the final mechanical properties such as impact strengthen. As shown by many researchers [36,44,65–69], the morphology of IPC obtained through scanning electronic microscopy (SEM) or transmission electronic microscopy (TEM) is a so-called ocean–island or core–shell structure where small amount of ethylene–propylene copolymers is well dispersed in iPP matrix. By pre-shearing, on the one hand, if the applied shear rate is sufficiently large, the crystallization rate of IPC will be significantly accelerated according to our experimental results, which is of great importance to production. However, on the other hand, the morphology of ocean–island or core–shell in IPC may be destroyed during the process and hard to recover leading to a depression on the final mechanical property. Therefore, practically, it is important to control the processing conditions of IPC to gain a good balance between crystallization enhancement and morphology destruction, both of which are crucial for final properties of the material.

4. Conclusion

In this study, a strong dependence of pre-shearing condition on crystallization kinetics of IPC was demonstrated. The IPC samples with various pre-shear histories were analyzed by nonisothermal crystallization and the results showed that both pre-shearing rate and duration time have a strong influence on T_p. With a sufficient high rate or enough long time, the T_p of IPC could be elevated by 10 °C at most. The isothermal crystallization behaviors were also studied and the overall crystallization kinetics analyzed by Avrami method reveals the different nucleation mechanisms between as-received IPC and pre-sheared IPC. By comparing $t_{1/2}$, it is showed that the pre-shearing process greatly accelerated the crystallization rate of IPC. The overwhelming changes of crystallization rate indicate a remarkable effect of pre-shearing on nucleation. Morphological evaluation during isothermal crystallization clearly confirmed the faster nucleation rate of pre-sheared IPC. Moreover, different from real nucleating agents, we found that pre-sheared samples showed relaxation behaviors under various annealing conditions.

At industrial level, to master the relationship between external flow field and internal crystallization, behaviors of polymer is both crucial and meaningful. As an important and complex polymer material, IPC showed a large response and long memory to pre-shearing. Therefore, it is possible to control the crystallization behaviors of IPC in practical processing.

Acknowledgements

We gratefully acknowledge the financial support from the National Natural Science Foundation of China (Grant Nos. 50673021, 20874017), the National Basic Research Program of China (G2005CB623803) and the Hi-Tech Research & Development Program of China (2007AA03Z450) and the Guangdong-MOE Special Fund (Grant No. 2007A090302091).

Appendix. Supplementary data

Supplementary data associated with this article can be found in the online version, at doi:10.1016/j.polymer.2008.10.054.

References

[1] Choudhary V, Varma HS, Varma IK. Polymer 1991;32:2534.
[2] Dorazio L, Mancarella C, Martuscelli E, Sticotti G, Massari P. Polymer 1993; 34:3671.
[3] McNally T, McShane P, Nally GM, Murphy WR, Cook M, Miller A. Polymer 2002;43:3785.
[4] Pang Y, Dong X, Zhang X, Liu K, Chen E, Han CC, et al. Polymer 2008;49:2568.
[5] Varga J. J Macromol Sci Phys 2002;B41:1121.
[6] Tjong SC, Shen JS, Li RKY. Polym Eng Sci 1996;36:100.
[7] Zhao S, Cai Z, Xin Z. Polymer 2008;49:2745.
[8] Yu TC. Polym Eng Sci 2001;41:656.
[9] Galli P, Haylock JC. Prog Polym Sci 1991;16:443.
[10] Simonazzi T, Cecchin G, Mazzullo S. Prog Polym Sci 1991;16:303.
[11] Urdampilleta I, Gonzalez A, Iruin JJ, de la Cal JC, Asua JM. Macromolecules 2005;38:2795.
[12] Mirabella FM. Polymer 1993;34:1729.
[13] Chai CK, Auzoux Q, Randrianatoandro H, Navard P, Haudin JM. Polymer 2003;44:773.
[14] Varga J, Karger–Kocsis J. J Polym Sci Part B Polym Phys 1996;34:657.
[15] Janeschitz-Kriegl H, Eder G. J Macromol Sci Part B Phys 2007;46:591.
[16] Isayev AI, Chan TW, Shimojo K, Gmerek M. J Appl Polym Sci 1995;55:807.
[17] Kumaraswamy G, Issaian AM, Kornfield JA. Macromolecules 1999;32:7537.
[18] Somani RH, Hsiao BS, Nogales A, Srinivas S, Tsou AH, Sics I, et al. Macromolecules 2000;33:9385.
[19] Somani RH, Hsiao BS, Nogales A, Fruitwala H, Srinivas S, Tsou AH. Macromolecules 2001;34:5902.
[20] Kumaraswamy G, Kornfield JA, Yeh FJ, Hsiao BS. Macromolecules 2002; 35:1762.
[21] Kumaraswamy G, Verma RK, Issaian AM, Wang P, Kornfield JA, Yeh F, et al. Polymer 2000;41:8931.
[22] Chai CK, Dixon NM, Gerrard DL, Reed W. Polymer 1995;36:661.
[23] Li LB, de Jeu WH. Macromolecules 2003;36:4862.
[24] Azzurri F, Alfonso GC. Macromolecules 2005;38:1723.
[25] Nogales A, Hsiao BS, Somani RH, Srinivas S, Tsou AH, Balta-Calleja FJ, et al. Polymer 2001;42:5247.
[26] Gutierrez MCG, Alfonso GC, Riekel C, Azzurri F. Macromolecules 2004;37:478.
[27] Sun T, Chen F, Dong X, Han CC. Polymer 2008;49:2717.
[28] Somani RH, Yang L, Zhu L, Hsiao BS. Polymer 2005;46:8587.
[29] Byelov D, Panine P, Remerie K, Biemond E, Alfonso GC, de Jeu WH. Polymer 2008;49:3076.
[30] Eder G, Janeschitzkriegl H, Liedauer S. Prog Polym Sci 1990;15:629.
[31] Zuidema H, Peters GWM, Meijer HEH. Macromol Theory Simul 2001;10:447.
[32] Doufas AK, McHugh AJ, Miller C. J Non-Newtonian Fluid Mech 2000;92:27.

[33] Doufas AK, McHugh AJ, Miller C, Immaneni A. J Non-Newtonian Fluid Mech 2000;92:81.
[34] Coppola S, Balzano L, Gioffredi E, Maffettone PL, Grizzuti N. Polymer 2004;45:3249.
[35] Coppola S, Grizzuti N, Maffettone PL. Macromolecules 2001;34:5030.
[36] Tan HS, Li L, Chen ZN, Song YH, Zheng Q. Polymer 2005;46:3522.
[37] Zheng Q, Shangguan Y, Yan SK, Song YH, Peng M, Zhang QB. Polymer 2005;46:3163.
[38] Tribout C, Monasse B, Haudin JM. Colloid Polym Sci 1996;274:197.
[39] Zhang X, Man X, Han CC, Yan D. Polymer 2008;49:2368.
[40] Cheng BJ, Zhou CX, Yu W, Sun XY. Polym Test 2001;20:811.
[41] Mallette JG, Soberanis RR. Polym Eng Sci 1998;38:1436.
[42] Nielsen LE. Polymer rheology. New York: Marcel Dekker; 1977.
[43] Nakajima N, Harrell ER. Rubber Chem Technol 1979;52:9.
[44] Chen Y, Chen Y, Chen W, Yang D. Eur Polym J 2007;43:2999.
[45] Page KA, Schilling GD, Moore RB. Polymer 2004;45:8425.
[46] Hoffman JD, Miller RL. Polymer 1997;38:3151.
[47] Godovsky YK, Slonimsk Gl. J Polym Sci Part B Polym Phys 1974;12:1053.
[48] Clark EJ, Hoffman JD. Macromolecules 1984;17:878.
[49] Hoffman JD, Miller RL, Marand H, Roitman DB. Macromolecules 1992; 25:2221.
[50] Binsberg FI, Delange BGM. Polymer 1970;11:309.
[51] Wlochowicz A, Eder M. Polymer 1981;22:1285.
[52] Tjong SC, Bao SP. J Polym Sci Part B Polym Phys 2005;43:253.
[53] Xu WB, He PS. Polym Eng Sci 2001;41:1903.
[54] Muller AJ, Arnal ML. Prog Polym Sci 2005;30:559.
[55] Lorenzo AT, Arnal ML, Sanchez JJ, Muller AJ. J Polym Sci Part B Polym Phys 2006;44:1738.
[56] Fillon B, Wittmann JC, Lotz B, Thierry A. J Polym Sci Part B Polym Phys 1993;31:1383.
[57] Xie YC, Zhang Q, Fan XD. J Appl Polym Sci 2003;89:2686.
[58] Kong J, Fan XD, Xie YC, Qiao WQ. J Appl Polym Sci 2004;94:1710.
[59] Mang MQ, Wanke SE. Polym Eng Sci 2003;43:1878.
[60] Muller AJ, Arnal ML, Spinelli AL, Canizales E, Puig CC, Wang H. Macromol Chem Phys 2003;204:1497.
[61] Starck P, Rajanen K, Lofgren B. Thermochim Acta 2002;395:169.
[62] Zhang FJ, Fu Q, Lu TJ, Huang HY, He TB. Polymer 2002;43:1031.
[63] Arnal ML, Balsamo V, Ronca G, Sanchez A, Muller AJ, Canizales E, et al. J Therm Anal Calorim 2000;59:451.
[64] Muller AJ, Hernandez ZH, Arnal ML, Sanchez JJ. Polym Bull 1997;39:465.
[65] Chen Y, Chen Y, Chen W, Yang DC. Polymer 2006;47:6808.
[66] Ito J, Mitani K, Mizutani Y. J Appl Polym Sci 1992;46:1221.
[67] Yokoyama Y, Ricco T. J Appl Polym Sci 1997;66:1007.
[68] Cai HJ, Luo XL, Ma DZ, Wang JM, Tan HS. J Appl Polym Sci 1999;71:93.
[69] Laupretre F, Bebelman S, Daoust D, Devaux J, Legras R, Costa JL. J Appl Polym Sci 1999;74:3165.